Quantifying the Sensitivity of Sea Level Change in Coastal Localities to the Geometry of Polar Ice Mass Flux

JERRY X. MITROVICA

Earth and Planetary Sciences, Harvard University, Cambridge, Massachusetts

CARLING C. HAY

Earth and Environmental Sciences, Boston College, Chestnut Hill, Massachusetts

ROBERT E. KOPP

Department of Earth and Planetary Sciences and Institute of Earth, Ocean, and Atmospheric Sciences, Rutgers, The State University of New Jersey, New Brunswick, New Jersey

CHRISTOPHER HARIG

Department of Geosciences, The University of Arizona, Tucson, Arizona

KONSTANTIN LATYCHEV

Earth and Planetary Sciences, Harvard University, Cambridge, Massachusetts

(Manuscript received 12 July 2017, in final form 15 November 2017)

ABSTRACT

It has been known for over a century that the melting of individual ice sheets and glaciers drives distinct geographic patterns, or fingerprints, of sea level change, and recent studies have highlighted the implications of this variability for hazard assessment and inferences of meltwater sources. These studies have computed fingerprints using simplified melt geometries; however, a more generalized treatment would be advantageous when assessing or projecting sea level hazards in the face of quickly evolving patterns of ice mass flux. In this paper the usual fingerprint approach is inverted to compute site-specific sensitivity kernels for a global database of coastal localities. These kernels provide a mapping between geographically variable mass flux across each ice sheet and glacier and the associated static sea level change at a given site. Kernels are highlighted for a subset of sites associated with melting from Greenland, Antarctica, and the Alaska–Yukon–British Columbia glacier system. The latter, for example, reveals an underappreciated sensitivity of ongoing and future sea level change along the U.S. West Coast to the geometry of ice mass flux in the region. Finally, the practical utility of these kernels is illustrated by computing sea level predictions at a suite of sites associated with annual variability in Greenland ice mass since 2003 constrained by satellite gravity measurements.

1. Introduction

A number of factors contribute to the geographic variability of sea level change, including changes in ocean dynamics, thermosteric effects, land water storage, local vertical land movement due to tectonics and sediment compaction, and the melting of glaciers and ice sheets (Milne et al. 2009), all of which are superimposed on large-scale, long-term geographic trends associated with ongoing glacial isostatic adjustment (Peltier 2004;

Denotes content that is immediately available upon publication as open access.

Supplemental information related to this paper is available at the Journals Online website: https://doi.org/10.1175/JCLI-D-17-0465.s1.

Corresponding author: Jerry X. Mitrovica, jxm@eps.harvard.edu

DOI: 10.1175/JCLI-D-17-0465.1

Lambeck et al. 2014). The impact of modern melting of ice sheets and glaciers on static sea level has been a particular focus of study (Clark and Lingle 1977; Clark and Primus 1987; Conrad and Hager 1997; Mitrovica et al. 2001; Plag 2006; Tamisiea et al. 2001; Bamber and Riva 2010; Mitrovica et al. 2011; Brunnabend et al. 2015; Spada and Galassi 2016). This interest is driven, in part, by the expectation that this contribution will become increasingly dominant across the twenty-first century (Church et al. 2013; Kopp et al. 2014). A comparative study of static and dynamic effects suggests that the former will dominate the latter over most of the world oceans when ice melt exceeds ~20 cm of equivalent global mean sea level (GMSL) rise, and at much lower levels of melt at sites close to areas of ice mass flux (Kopp et al. 2010). Moreover, the deformational, gravitational, and rotational effects of ice mass flux on static sea level are well understood (Farrell and Clark 1976). Mass flux from each ice sheet and glacier will drive a unique geographical pattern of static sea level change, and these so-called fingerprints (Plag and Jüttner 2001) now play an important role in analyses of modern sea level records (Hay et al. 2015; Brunnabend et al. 2015; Spada and Galassi 2016) and assessments of regional sea level hazards (Slangen et al. 2012).

A standard global calculation based on the assumption of uniform, rapid melting from the Greenland Ice Sheet (GIS) equivalent in volume to a GMSL rise of 1 mm yr^{-1} highlights the physical effects that contribute to sea level fingerprints (see Fig. S1 in the online supplemental material at the Journals Online website: https://doi.org/10.1175/JCLI-D-17-0465.s1.). Within a zone that extends ~2000 km from an ice sheet, sea level will fall as a consequence of both the decreased gravitational pull of the diminished ice sheet and the elastic uplift of the crust in response to the ice unloading. At the edges of Greenland, this sea level fall can reach ~10 mm yr^{-1}, an order of magnitude larger than (and of opposite sign to) the equivalent GMSL rise. The predicted sea level change generally increases at progressively greater distance from the ice sheet, with maximum values of ~1.4 mm yr^{-1} in regions far from the melting ice. There are other physical effects active in the prediction, including meltwater loading of the oceans, which produces the coastline-parallel pattern of the contours (e.g., Australia, southern South America), and the feedback on sea level of the load-induced perturbation in Earth rotation (an ~1° Myr^{-1} reorientation of the north rotation axis toward Greenland per mm yr^{-1} of equivalent GMSL rise; Mitrovica et al. 2006), which accounts for a portion of the azimuthal asymmetry in the far field of the ice sheet. We note that, at this level of melt, the sea level prediction is linearly related to the ice volume change, and so the results in Fig. 1 can be scaled to consider the sea level change associated with mass fluxes of different magnitude and sign as long as the geometry of the mass flux remains the same.

Published fingerprints are relatively few in number and are, with few exceptions (Bamber and Riva 2010; Mitrovica et al. 2011), generally based on highly simplified geometries of ice mass flux (e.g., a uniform mass loss across the ice sheet, as in Fig. 1) (Clark and Lingle 1977; Clark and Primus 1987; Conrad and Hager 1997; Mitrovica et al. 2001; Plag 2006; Brunnabend et al. 2015; Spada and Galassi 2016). This simplification limits the incorporation of more realistic ice-melt scenarios into regional sea level projections (Sweet et al. 2017) and, more generally, the quantitative assessment of the sensitivity of local sea level to mass flux within different sectors of ice sheets and large glaciers systems. In this paper, we describe a generalized approach to fingerprinting that overcomes these limitations and provides the scientific community and coastal stakeholders with a tool to compute site-specific sea level changes for arbitrary melt scenarios, thereby providing insight into how sensitive these predictions are to changes in the location of melt.

2. Methods

For rapid ice mass changes, fingerprints are generally predicted assuming that the solid Earth response is elastic and accurately captured using a model of structure that varies with depth alone (Dziewonski and Anderson 1981). Large-scale lateral variations in elastic and density structure within Earth's mantle inferred from seismic tomography are small and impact fingerprints on the order of ~1% (Mitrovica et al. 2011). Inhomogeneities in crustal structure can perturb the elastic response to surface mass loading with spatial scale <2500 km^2 by ~10%, but this perturbation is relatively localized to the region of loading (Dill et al. 2015). Moreover, viscous deformation may be ignored for ice mass flux over time scales less than a few centuries, with the exception of sites local to melting in areas of very low (~10^{18} Pa s) viscosity within the shallow sublithospheric mantle. Areas where viscous effects of this kind have been considered include Alaska (James et al. 2009), Iceland (Auriac et al. 2013), Patagonia (Richter et al. 2016), eastern Greenland (Khan et al. 2016), the Antarctic Peninsula (Nield et al. 2014), and the West Antarctic (Hay et al. 2017). Under the above assumptions, the theoretical formulation governing gravitationally self-consistent relative sea level (SL) change on a rotating Earth can be expressed in terms of elastic Love number theory (Farrell and Clark 1976; Kendall et al. 2005).

In the case where the perimeter of any grounded, marine-based ice cover does not change, and global shoreline geometry remains fixed, SL is linearly related to the ice load (Farrell and Clark 1976) and one can thus express the SL change at a site r_o in the following form:

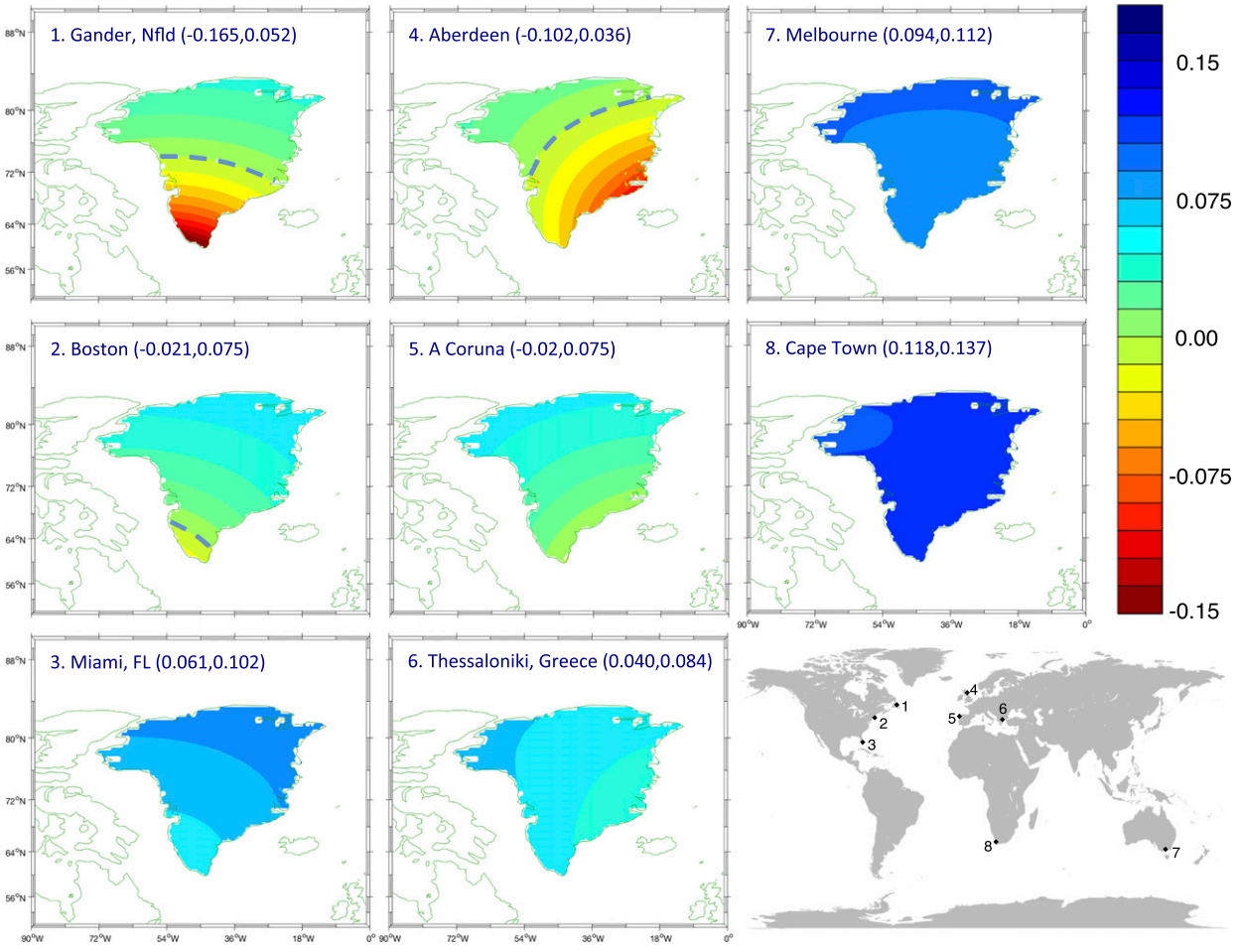

FIG. 1. Sea level sensitivity kernels over Greenland for selected coastal sites. Dimensionless sea level sensitivity kernels, $-K_o^*(\theta, \phi)$ [Eq. (2)], over Greenland for (left) sites along the east coast of North America, (middle) Europe, and (right) in the far field of the GIS. Location of sites is given on map at bottom right. Labels on each frame provide the minimum and maximum values of each kernel. The dashed lines superimposed on the kernels for sites 1, 2, and 4 indicate the zero contour.

$$\mathrm{SL}(r_o) = \iint_{\Omega} \rho_I I(\theta,\phi) K_o(\theta,\phi)\, d\Omega, \tag{1}$$

where ρ_I is the density of ice, I is the change in ice height, K_o is the sea level sensitivity kernel for the site r_o, ($\mathrm{m\,kg^{-1}}$), θ and ϕ are the colatitude and east longitude, and the integral is taken over the surface area of Earth. This equation may be simplified to

$$\mathrm{SL}(r_o) = \iint_{\Omega_u} I(\theta,\phi) K_o^*(\theta,\phi)\, d\Omega_u, \tag{2}$$

where the integration is now performed over the unit sphere (Ω_u), the dimensionless kernel K_o^* is defined as

$$K_o^*(\theta,\phi) = \rho_I K_o(\theta,\phi) a^2, \tag{3}$$

and a is the radius of Earth. Following Eq. (3), each site on Earth's surface will have an associated sea level sensitivity kernel, and with this kernel one can compute the sea level change at the site in response to a geometry, $I(\theta, \phi)$, of ice mass change.

The sensitivity kernel $K_o^*(\theta, \phi)$ can be constructed using numerical perturbation procedures (e.g., Mitrovica and Peltier 1991). For example, to compute the value of the kernel at a location (θ_i, ϕ_i), one can run a gravitationally self-consistent sea level fingerprint simulation in which an ice loading is applied that is spatially localized to (θ_i, ϕ_i). If we denote this loading as $I_i(\theta, \phi)$ and the sea level change at r_o computed using this loading as $\mathrm{SL}_i(r_o)$, then using these expressions in Eq. (2) yields the following approximation:

$$K_o^*(\theta_i,\phi_i) \approx \frac{\mathrm{SL}_i(r_o)}{\iint_{\Omega_u} I_i(\theta,\phi)\, d\Omega_u}. \tag{4}$$

In practice, we solve a large number of gravitationally self-consistent sea level simulations in which the location of the localized loading $I_i(\theta, \phi)$ is systematically varied to sample any region characterized by glacial ice cover [e.g., the GIS, the Antarctic Ice Sheet (AIS), or any glacier system]. In each simulation, the sea level change is computed at a large set of coastal sites r_o. For each of the latter sites, the kernel K_o^* can then be computed over the regions of ice cover.

In computing the kernels discussed below, we adopt localized ice unloadings I_i that shave a thin layer of ice from any region of ice cover. These loads have a parabolic vertical cross section, circular horizontal cross section, a peak height of 1 m, and a radius of 0.6°. The radius is chosen to be consistent with the spherical harmonic truncation at degree and order 512 adopted in our sea level calculations (Kendall et al. 2005), and the height ensures that the perturbation in the sea level prediction is significantly higher than the numerical noise in the calculation. We computed the sea level sensitivity kernel for ~740 tide gauge sites in the Permanent Service for Mean Sea Level (PSMSL) database (Holgate et al. 2013), and these are provided online at https://doi.org/10.5281/zenodo.1170110.

Since only a thin layer of ice is removed, the kernels we have computed are valid for the case in which there is no significant retreat of grounded, marine-based ice cover or changes in global shoreline geometry. To derive kernels valid in the case of the retreat of grounded, marine-based ice, the localized ice unloading I_i would have to be sufficient to remove the full column of ice and an additional sea level signal associated with crustal rebound of the exposed marine-based sector would have to be modeled (Kendall et al. 2005; Gomez et al. 2010). In this case, or in the case of time-varying shorelines, sea level changes are not strictly linearly related to ice load changes and an alternate form of Eq. (1) may have to be considered.

3. Results and discussion

Sensitivity kernels within Greenland for a set of widely distributed sites are shown in Fig. 1 (site locations are given at bottom right). As an example, consider the kernel for Gander, Newfoundland. The site is situated relatively close to Greenland, and melting anywhere in the southern sector of the GIS (any melting south of the dashed line on the figure) will produce a sea level fall (i.e., Gander is within ~2000 km of this sector). Melting in the northern sector of the ice sheet will, in contrast, lead to a sea level rise. Moreover, as indicated by the minimum and maximum values labeled on the figure, mass flux in the far north of the GIS will produce a sea level rise at Gander that is ~1/3 the magnitude of the sea level fall that would occur following an equivalent mass flux at the southern tip of the ice sheet. Moving farther down the East Coast of North America, Boston will experience a sea level rise following melting of any part of the GIS with the exception of the southern tip of the ice sheet. Miami is sufficiently far from the GIS that melting anywhere within the ice sheet will produce a sea level rise at the site. It is interesting to note, however, that the kernel for Miami indicates that the predicted sea level rise can vary by nearly a factor of 2 depending on where the mass flux occurs within the GIS.

The sea level sensitivity kernels for the three European sites (middle column, Fig. 1) show the same trend toward more positive values as one considers locations at progressively farther distances from the GIS. The main difference evident in a comparison of the left and middle columns of Fig. 1 is the orientation of the contours. In both cases, the contours are oriented along great circles joining the observation site and the location of melt within the GIS (i.e., toward the north-northeast to south-southwest in the case of North American sites and northwest to southeast for the European sites). Finally, both Melbourne and Cape Town are at great distance from the GIS, and the kernels indicate that the sea level change they will experience in response to melting of the ice sheet will be relatively insensitive to the location of melting.

Sensitivity kernels for Antarctica (Fig. 2) show similar near-field versus far-field patterns. There is no site in the Antarctic that is within ~2000 km of Cape Town or Melbourne, and thus the kernels for these sites are positive throughout the entire AIS; that is, regardless of where melting occurs within the AIS, Cape Town and Melbourne will always experience a sea level rise in response to this melting. Nevertheless, these kernels do show significant spatial variability, indicating that the magnitude of sea level rise at the two sites will depend strongly on the geometry of melting, even within the West Antarctic Ice Sheet (WAIS). As an example, in the case of Melbourne, sea level rise following melting from the northern tip of the Antarctic Peninsula will be ~2 times higher than the rise if the equivalent mass flux occurs in Marie Byrd Land, where it abuts the Ross Ice Shelf. Similarly, melting in Marie Byrd Land will drive a sea level rise in Cape Town that is ~2 times higher than an equivalent melt event in Queen Maud Land in the East Antarctic. As in Fig. 1, the kernels for both sites are characterized by gradients that lie along a great circle joining the site and the ice sheet, in this case the AIS. Finally, Miami is in the far field of the AIS and thus the sea level rise it would experience in response to melting within the AIS is less sensitive to the location of the

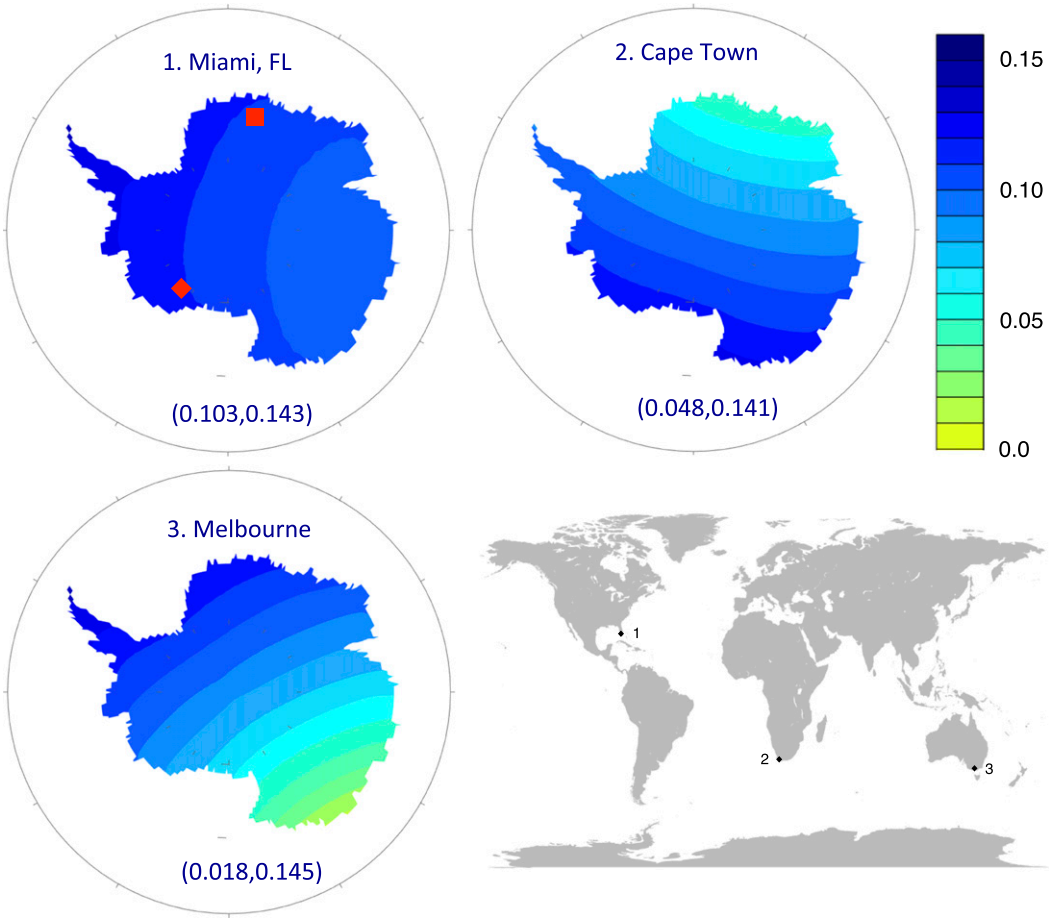

FIG. 2. As in Fig. 1, but for kernels over Antarctica. The red diamond and square in the top left frame show the locations of two sites referred to in the main text, Marie Byrd Land and Queen Maud Land, respectively.

melting, although the associated kernel for the site still varies by about 30% across the AIS.

As an example of sea level sensitivity kernels for glacier systems, we next consider kernels for five sites along the Pacific coast of the United States and Mexico for the case of melting across the Alaska–Yukon–British Columbia glacier system (Fig. 3). Sites 1–5 in Fig. 3 are located at progressively greater distances from this system, and thus the trend in the kernels is toward more positive values as one moves southward along the coast. Seattle, the northernmost site, will experience a sea level fall in response to melting in the glacier system regardless of where the melting occurs, but the magnitude of the resulting sea level fall will be a very strong function of the latitudinal location of the glacier melting. It is perhaps more surprising that a site as far south as San Diego will experience a sea level fall if melting is localized to the southernmost ice fields of the glacier system (the location of the Ketchikan Icefield is shown on the kernel for San Diego). In any event, the pattern of sea level change along the entire west coast of the United States and Mexico will be sensitive to the geometry of melting within the Alaska–Yukon–British Columbia glacier system, which varies on multiple time scales (Harig and Simons 2016).

Taken together, the results in Figs. 1–3 demonstrate that the sea level sensitivity kernels provide a more nuanced measure of the sensitivity of individual sites to melting within an ice sheet than a sea level fingerprint based on the assumption of uniform melting of the ice sheet (e.g., Fig. S1). We emphasize that to predict the sea level change due to ice melting at any site one simply multiplies the kernel by the ice mass flux (whether based on constraints of past or ongoing ice mass changes, or projections of future changes) and integrates the product.

As a simple illustration of the utility of the kernels, we used them to compute changes in sea level at the eight coastal sites shown in Fig. 1 driven by GIS mass flux over the past decade. Harig and Simons (2012) used a

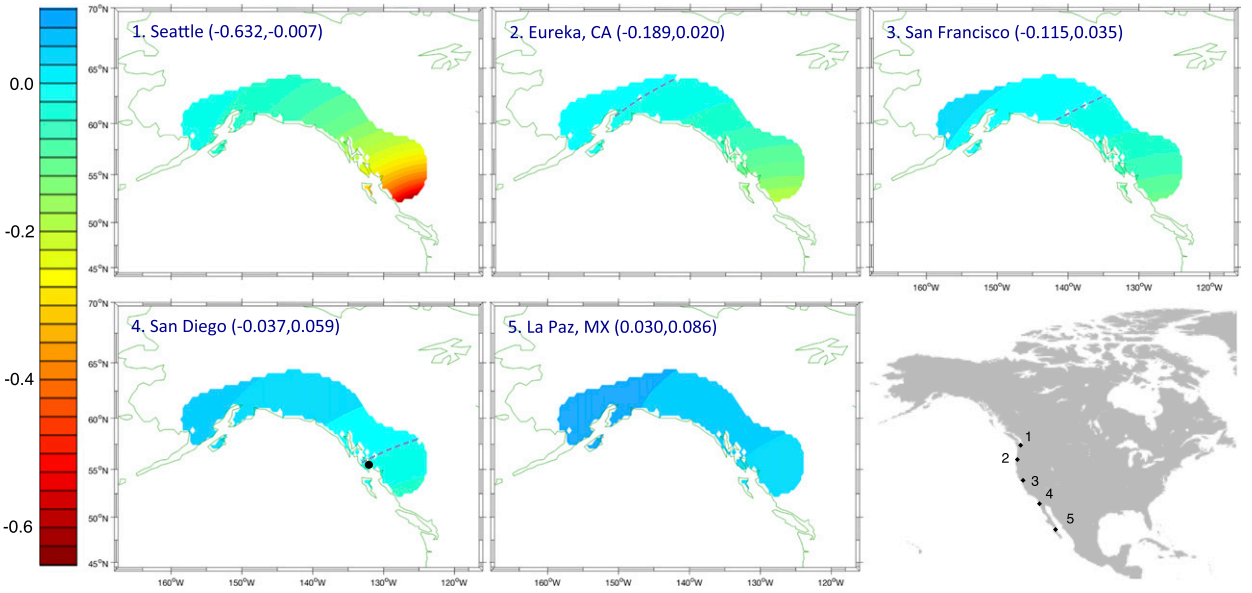

FIG. 3. As in Fig. 2, but for kernels over coastal Alaska. Sites are located at progressive distance from Alaska along the east coast of North America. The black circle on the San Diego kernel shows the location of the Ketchikan Icefield in southernmost Alaska.

truncated basis set of 20 spherical Slepian functions to invert monthly satellite gravimetry measurements from GRACE and reconstruct ice mass changes over Greenland. By fitting polynomial trends to each of their Slepian function expansion coefficient time series, they estimated how the geometry of ice flux evolved over time. [See Khan et al. (2015) for a review of other geodetic investigations of the recent mass balance of the GIS.] We used a 2003–15 update of these yearly resolved maps of mass changes (Fig. S2) to compute both yearly and cumulative sea level changes at the eight sites (Figs. 4a and 4c, respectively). The black line in Fig. 4a is the global mean sea level change associated with each year of ice mass flux. We also computed yearly sea level changes normalized by this GMSL trend (Fig. 4b).

Over the period 2003–15, the mass loss from Greenland peaked in 2010 in the analysis of Harig and Simons (2012) (Fig. 4a). The yearly sea level changes predicted for the two sites in the far field of Greenland, namely Melbourne and Cape Town, follow the trend in the GMSL change (see also Fig. 4b), with the latter site peaking 25% higher than the former (and 20% higher than the GMSL change). As one consider sites progressively closer to the GIS, for example the triplet of sites Miami, Boston, and Gander (or Thessaloniki, A Coruña, and Aberdeen), the predictions diverge by increasing amounts from the yearly GMSL change. These curves also diverge from a simple scaling of the GMSL trend (Fig. 4b), which reflects the evolving geometry of the GIS mass flux and associated sea level change. An example is the prediction for Aberdeen, which shows a nearly constant yearly sea level fall over the 12-yr time window we are considering, and a normalized sea level change that varies from -0.7 in 2003 to ~ -0.2 after 2008. Finally, the magnitude of the cumulative sea level rise varies by a factor of ~ 4 from Boston or A Coruña to Cape Town (Fig. 4c).

The kernels in Figs. 1–3 were computed under the assumption that Earth's response to changing surface mass loads is purely elastic. This assumption will introduce an error in sea level predictions at sites close to regions in which ice mass flux overlies low-viscosity mantle (e.g., Alaska, Iceland, Patagonia, eastern Greenland, the Antarctic Peninsula, and the West Antarctic). To explore this issue in the context of Fig. 3, we performed two simulations in which we modeled uniform melting across the Alaskan glacier system over a period of 20 yr. The first simulation adopted an elastic Earth model, and the second adopted a 3D mantle viscosity field inferred from the seismic model S40RTS (Ritsema et al. 2011) using the method described in Austermann et al. (2013). The latter was characterized by mantle viscosity values below Alaska as low as 10^{18} Pa s (Fig. S3a). The perturbation in the sea level prediction introduced by viscous effects (i.e., 3D minus 1D calculation), expressed as a percentage of the GMSL change associated with the melting, was 7% at Seattle, 3% at Eureka, 2% at San Francisco, and less than 1% at both San Diego and La Paz (Fig. S3b). Similar levels of perturbation due to low-viscosity structure have been predicted for sites outside the Antarctic in the case of

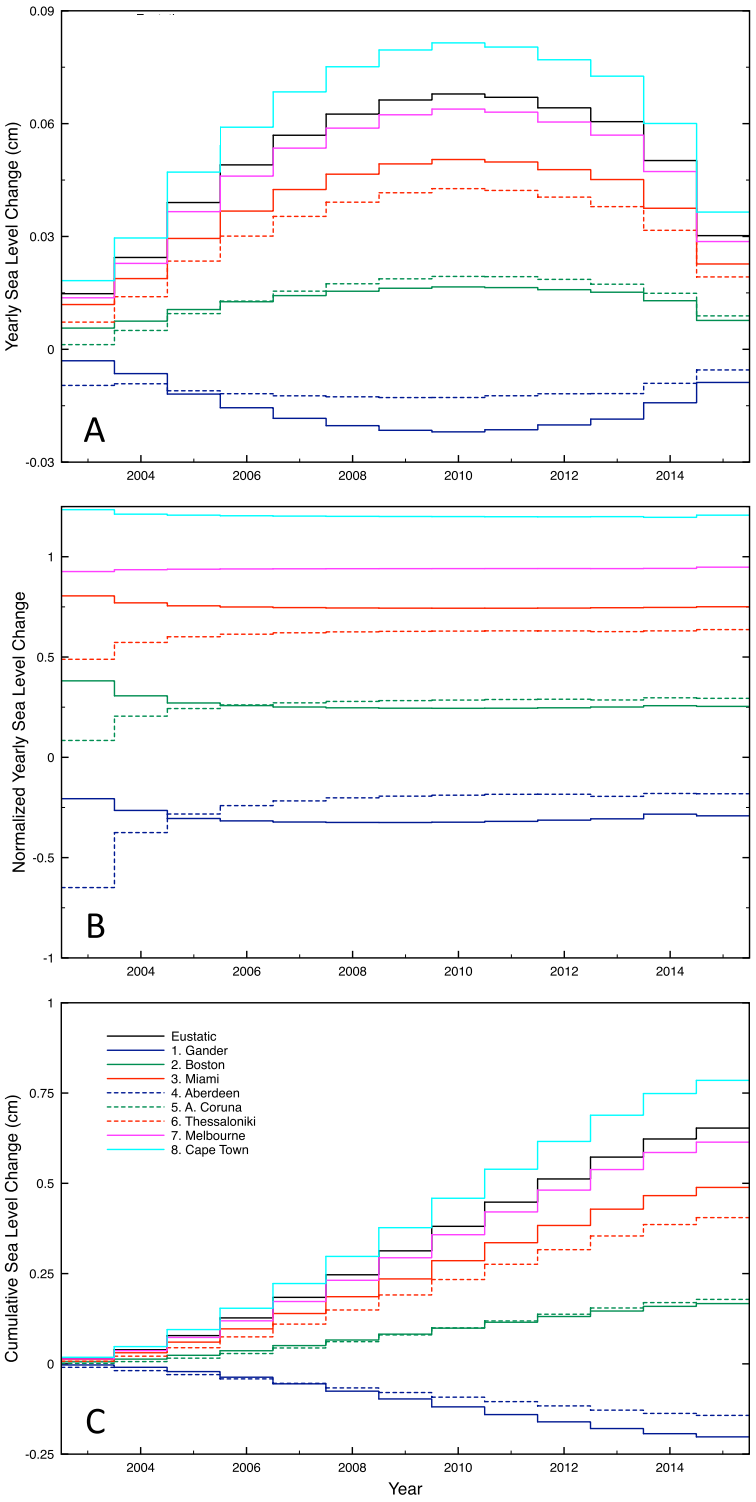

FIG. 4. Computed yearly sea level change at selected coastal sites due to ice mass flux from Greenland. (a) Sea level change each year from 2003 to 2015 computed using the kernel approach described in the text [see Eq. (1) and Fig. 1] and ice mass changes shown in Fig. S2. The thick black line is the global mean sea level ("eustatic") change during each year associated with the ice mass history. (b) Yearly sea level changes at each coastal site in (a) normalized by the GMSL change [black curve in (a)]. (c) Cumulative sea level change at the eight coastal sites [i.e., integral of the curves in (a)].

melting from the WAIS (Hay et al. 2017). These results suggest that nonnegligible viscous effects on sea level fingerprints will be localized to the regions listed above.

4. Conclusions

We have described a flexible, kernel-based approach to determining sea level changes at a large, globally distributed set of coastal sites driven by polar ice mass variations. The approach assumes that melting does not significantly alter the perimeter of any grounded, marine-based ice cover or the geometry of global shorelines; however, as we have discussed, the sensitivity kernels can be extended (in a linearized manner) to treat these issues. The kernels also assume that the response of a solid Earth to the surface mass change is purely elastic, but we have demonstrated that the impact of viscous effects on sea level fingerprints and associated kernels will be largely localized to sites close to zones in which ice melting overlies low viscosity mantle (see also Hay et al. 2017). In the case where viscous effects are important over global scales (e.g., if one considers polar ice mass flux with significantly longer, say millennial, time scales), the kernel approach described here is not appropriate and must be extended because a time convolution would be required to compute the sea level response to the surface mass loading. A generalized treatment that incorporates both time varying shorelines and viscous effects is left for future work.

We note once more that the kernels have been computed using a numerical scheme in which ice mass is perturbed in the form of discs of radius 0.6° (~66 km). This raises the issue of whether suitably interpolated versions of these kernels may be used to compute the sea level response in the case of melt models of higher resolution. The accuracy of such predictions is guaranteed for sites outside the zone of melting (e.g., Spada et al. 2012). However, we believe the interpolated kernels would also be accurate for predictions at sites within the zones of (high resolution) melting given the smooth, long wavelength nature of the kernels in Figs. 1–3.

The power of the kernel method is its flexibility. One can use the approach to predict sea level changes at a site of interest for any number of projections of future ice mass changes without the necessity of solving the complex integral equation that governs gravitationally self-consistent sea level fingerprints (Farrell and Clark 1976; Clark and Lingle 1977; Clark and Primus 1987; Conrad and Hager 1997; Mitrovica et al. 2001; Tamisiea et al. 2001; Kendall et al. 2005; Plag 2006; Bamber and Riva 2010; Gomez et al. 2010; Mitrovica et al. 2011; Slangen et al. 2012; Brunnabend et al. 2015; Hay et al. 2015, 2017; Spada and Galassi 2016). Indeed, the solutions to the sea level equation are embedded a priori in the calculation of the kernels. Kernels for approximately 740 sites in the PSMSL database are provided for geographic regions covering Greenland, the Antarctic, and the Alaska–Yukon–British Columbia glacier system.

Acknowledgments. Funding was provided by Harvard University, NASA Awards NNX17AE17G (JXM, KL), NNX17AE18G (CH), and 80NSSC17K0698 (REK, JXM), and NSF Award ICER-1663807 (REK). We thank Ophelia Crawford and three anonymous reviewers for insightful comments related to this work.

REFERENCES

Auriac, A., K. H. Spaans, F. Sigmundsson, A. Hooper, P. Schmidt, and B. Lund, 2013: Iceland rising: Solid Earth response to ice retreat inferred from satellite radar interferometry and viscoelastic modeling. *J. Geophys. Res.*, **118**, 1331–1344, https://doi.org/10.1002/jgrb.50082.

Austermann, J., J. X. Mitrovica, K. Latychev, and G. A. Milne, 2013: Barbados-based estimate of ice volume at Last Glacial Maximum affected by subducted plate. *Nat. Geosci.*, **6**, 553–557, https://doi.org/10.1038/ngeo1859.

Bamber, J., and R. Riva, 2010: The sea level fingerprint of recent ice mass fluxes. *Cryosphere*, **4**, 621–627, https://doi.org/10.5194/tc-4-621-2010.

Brunnabend, S. E., J. Schröter, R. Rietbroek, and J. Kusche, 2015: Regional sea level change in response to ice mass loss in Greenland, the West Antarctic and Alaska. *J. Geophys. Res. Oceans*, **120**, 7316–7328, https://doi.org/10.1002/2015JC011244.

Church, J. A., and Coauthors, 2013: Sea level change. *Climate Change 2013: The Physical Science Basis.* T. F. Stocker et al., Eds., Cambridge University Press, 1137–1216.

Clark, J. A., and C. S. Lingle, 1977: Future sea-level changes due to West Antarctic ice sheet fluctuations. *Nature*, **269**, 206–209, https://doi.org/10.1038/269206a0.

——, and J. A. Primus, 1987: Sea-level changes resulting from future retreat of ice sheets: An effect of CO_2 warming of the climate. *Sea-Level Changes*, M.-J. Tooley and I. Shennan, Eds., Institute of British Geographers, 356–370.

Conrad, C., and B. H. Hager, 1997: Spatial variations in the rate of sea level rise caused by present-day melting of glaciers and ice sheets. *Geophys. Res. Lett.*, **24**, 1503–1506, https://doi.org/10.1029/97GL01338.

Dill, R., V. Klemann, Z. Martinec, and M. Tesauro, 2015: Applying local Green's functions to study the influence of the crustal structure on hydrological loading displacements. *J. Geodyn.*, **88**, 14–22, https://doi.org/10.1016/j.jog.2015.04.005.

Dziewonski, A. M., and D. L. Anderson, 1981: Preliminary reference Earth model (PREM). *Phys. Earth Planet. Inter.*, **25**, 297–356, https://doi.org/10.1016/0031-9201(81)90046-7.

Farrell, W. E., and J. A. Clark, 1976: On postglacial sea level. *Geophys. J. Roy. Astron. Soc.*, **46**, 647–667, https://doi.org/10.1111/j.1365-246X.1976.tb01252.x.

Gomez, N., J. X. Mitrovica, M. E. Tamisiea, and P. U. Clark, 2010: A new projection of sea level change in response to collapse of

marine sectors of the Antarctic Ice Sheet. *Geophys. J. Int.*, **180**, 623–634, https://doi.org/10.1111/j.1365-246X.2009.04419.x.

Harig, C., and F. J. Simons, 2012: Mapping Greenland's mass loss in space and time. *Proc. Natl. Acad. Sci. USA*, **109**, 19 934–19 937, https://doi.org/10.1073/pnas.1206785109.

——, and ——, 2016: Ice mass loss in Greenland, the Gulf of Alaska, and the Canadian Archipelago: Seasonal cycles and decadal trends. *Geophys. Res. Lett.*, **43**, 3150–3159, https://doi.org/10.1002/2016GL067759.

Hay, C. C., E. Morrow, R. E. Kopp, and J. X. Mitrovica, 2015: Probabilistic reanalysis of twentieth-century global sea-level rise. *Nature*, **517**, 481–484, https://doi.org/10.1038/nature14093.

——, H. C. P. Lau, N. Gomez, J. Austermann, E. Powell, J. X. Mitrovica, L. Latychev, and D. A. Wiens, 2017: Sea-level fingerprints in a region of complex Earth structure: The case of WAIS. *J. Climate*, **30**, 1881–1892, https://doi.org/10.1175/JCLI-D-16-0388.1.

Holgate, S. J., and Coauthors, 2013: New data systems and products at the Permanent Service for Mean Sea Level. *J. Coast. Res.*, **29**, 493–504, https://doi.org/10.2112/JCOASTRES-D-12-00175.1.

James, T. S., E. J. Gowan, I. Wada, and K. Wang, 2009: Viscosity of the asthenosphere from glacial isostatic adjustment and subduction dynamics at the northern Cascadia subduction zone, British Columbia, Canada. *J. Geophys. Res.*, **114**, B04405, https://doi.org/10.1029/2008JB006077.

Kendall, R., J. X. Mitrovica, and G. A. Milne, 2005: On post-glacial sea-level—II. Numerical formulation and comparative results on spherically symmetric Earth models. *Geophys. J. Int.*, **161**, 679–706, https://doi.org/10.1111/j.1365-246X.2005.02553.x.

Khan, S. A., A. Aschwanden, A. A. Bjørk, J. Wahr, K. K. Kjeldsen, and K. H. Kjær, 2015: Greenland Ice Sheet mass balance: A review. *Rep. Prog. Phys.*, **78**, 046801, https://doi.org/10.1088/0034-4885/78/4/046801.

——, and Coauthors, 2016: Geodetic measurements reveal similarities between post–Last Glacial Maximum and present-day mass loss from the Greenland Ice Sheet. *Sci. Adv.*, **2**, e1600931, https://doi.org/10.1126/sciadv.1600931.

Kopp, R. E., J. X. Mitrovica, S. M. Griffies, J. Yin, C. C. Hay, and R. J. Stouffer, 2010: The impact of Greenland melt on regional sea-level: A partially coupled analysis of dynamic and static equilibrium effects. *Climate Change*, **103**, 619–625, https://doi.org/10.1007/s10584-010-9935-1.

——, R. M. Horton, C. M. Little, J. X. Mitrovica, M. Oppenheimer, D. J. Rasmussen, B. H. Strauss, and C. Tebaldi, 2014: Probabilistic 21st and 22nd century sea-level projections at a global network of tide gauge sites. *Earth's Future*, **2**, 287–306, https://doi.org/10.1002/2014EF000239.

Lambeck, K., H. Rouby, A. Purcell, Y. Sun, and M. Sambridge, 2014: Sea level and global ice volumes from the Last Glacial Maximum to the Holocene. *Proc. Natl. Acad. Sci. USA*, **111**, 15 296–15 303, https://doi.org/10.1073/pnas.1411762111.

Milne, G. A., W. R. Gehrels, C. W. Hughes, and M. E. Tamisiea, 2009: Identifying the causes of sea-level change. *Nat. Geosci.*, **2**, 471–478, https://doi.org/10.1038/ngeo544.

Mitrovica, J. X., and W. R. Peltier, 1991: A complete formalism for the inversion of post-glacial rebound data: Resolving power analysis. *Geophys. J. Int.*, **104**, 267–288, https://doi.org/10.1111/j.1365-246X.1991.tb02511.x.

——, M. E. Tamisiea, J. L. Davis, and G. A. Milne, 2001: Polar ice mass variations and the geometry of global sea level change. *Nature*, **409**, 1026–1029, https://doi.org/10.1038/35059054.

——, J. Wahr, I. Matsuyama, A. Paulson, and M. E. Tamisiea, 2006: Reanalysis of ancient eclipse, astronomic and geodetic data: A possible route to resolving the enigma of global sea level rise. *Earth Planet. Sci. Lett.*, **243**, 390–399, https://doi.org/10.1016/j.epsl.2005.12.029.

——, N. Gomez, E. Morrow, C. C. Hay, K. Latychev, and M. E. Tamisiea, 2011: On the robustness of predictions of sea level fingerprints. *Geophys. J. Int.*, **187**, 729–742, https://doi.org/10.1111/j.1365-246X.2011.05090.x.

Nield, G. A., and Coauthors, 2014: Rapid bedrock uplift in the Antarctic Peninsula explained by viscoelastic response to recent ice unloading. *Earth Planet. Sci. Lett.*, **397**, 32–41, https://doi.org/10.1016/j.epsl.2014.04.019.

Peltier, W. R., 2004: Global glacial isostasy and the surface of the ice-age Earth: The ICE-5G (VM2) model and GRACE. *Annu. Rev. Earth Planet. Sci.*, **32**, 111–149, https://doi.org/10.1146/annurev.earth.32.082503.144359.

Plag, H.-P., 2006: Recent relative sea-level trends: An attempt to quantify the forcing factors. *Philos. Trans. Roy. Soc.*, **364A**, 821–844, https://doi.org/10.1098/rsta.2006.1739.

——, and H. U. Jüttner, 2001: Inversion of global tide gauge data for present-day ice load changes. *Mem. Nat. Inst. Polar Res.* **54**, 301–318.

Richter, A., and Coauthors, 2016: Crustal deformation across the Southern Patagonia Icefield observed by GNSS. *Earth Planet. Sci. Lett.*, **452**, 206–215, https://doi.org/10.1016/j.epsl.2016.07.042.

Ritsema, J., A. Deuss, H. J. van Heijst, and J. H. Woodhouse, 2011: S40RTS: A degree-40 shear-velocity model for the mantle from new Rayleigh wave dispersion, teleseismic traveltime and normal-mode splitting function measurements. *Geophys. J. Int.*, **184**, 1223–1236, https://doi.org/10.1111/j.1365-246X.2010.04884.x.

Slangen, A. B. A., C. A. Katsman, R. S. W. van de Wal, L. L. A. Vermeersen, and R. E. M. Riva, 2012: Towards regional projections of twenty-first century sea-level change based on IPCC SRES scenarios. *Climate Dyn.*, **38**, 1191–1209, https://doi.org/10.1007/s00382-011-1057-6.

Spada, G., and G. Galassi, 2016: Spectral analysis of sea level during the altimetry era, and evidence for GIA and glacial melting fingerprints. *Global Planet. Change*, **143**, 34–49, https://doi.org/10.1016/j.gloplacha.2016.05.006.

——, G. Ruggieri, L.S. Sørensen, K. Nielsen, D. Melini, and F. Colleoni, 2012: Greenland uplift and sea level changes from ICESat observations and GIA modelling. *Geophys. J. Int.*, **189**, 1457–1474, https:/doi.org/10.1111/j.1365-246X.2012.05443.x.

Sweet, W. V., R. E. Kopp, C. P. Weaver, J. Obeysekera, R. M. Horton, E. R. Thieler, and C. Zervas, 2017: Global and regional sea level rise scenarios for the United States. NOAA Tech. Rep. NOS CO-OPS 083, 75 pp., http://apo.org.au/node/72441.

Tamisiea, M. E., J. X. Mitrovica, G. A. Milne, and J. L. Davis, 2001: Global geoid and sea level changes due to present-day ice mass fluctuations. *J. Geophys. Res.*, **106**, 30 849–30 863, https://doi.org/10.1029/2000JB000011.